

## Self-Assembled Gold Layers on Micropatterned Substrates for SERS Sensing of Rhodamine 6G

Lenzi J. Williams, Ph.D., Principal Research Scientist

Daniel Massey, Director of Lithography

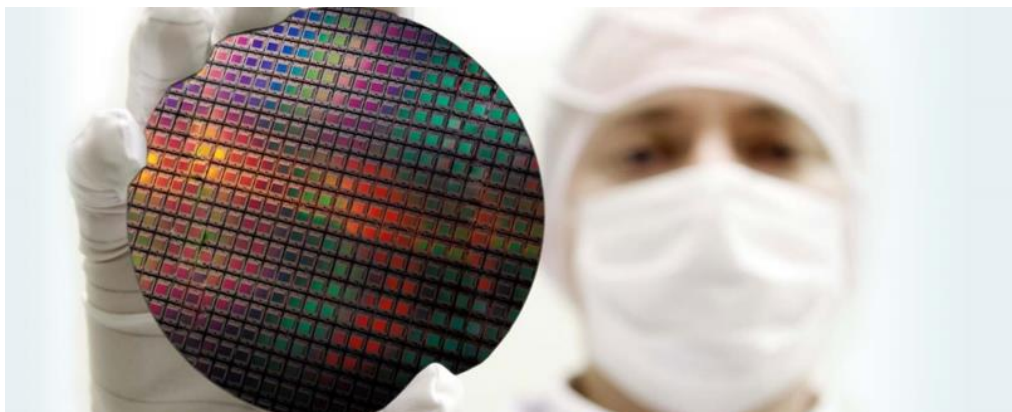
Natasha Davis, Supervisor of Lithography

### Introduction

Microstructure arrays are configurations of a number of periodically arranged optical elements with shape and size-dependent functionalities. Owing to the geometrically controlled features, microstructure arrays offer a wide variety of optical functions. Arrays with elements sized 0.5~50  $\mu\text{m}$  achieve superior performance mainly due to their refraction and reflection properties. Microstructures of these types are exploited to manufacture electronic products such as LCDs, cell phones, and televisions. Arrays with smaller element sizes, 0.5~5  $\mu\text{m}$ , achieve optical performance mainly due to their interference and diffraction reflection properties used for example in diffraction grating related technologies.

Sensing applications also greatly benefit from ordered microstructures operating as optical transducers of mechanical, chemical, and thermal signals.<sup>1,2,3</sup> Specifically, gold coating the arrayed features to perform surface enhanced Raman scattering (SERS) measurements improves the sensitivity and the detection limit of analyte sensing.<sup>4</sup> As a SERS substrate, micropatterned surfaces have an increased surface area-to-volume ratio when compared to flat substrates.

Here, we have applied a wet chemical approach for the self-assembly of gold nanoparticles on micropatterned substrates for the detection of the common Raman reporter molecule, Rhodamine 6G (R6G). R6G SERS detection was also carried out on a gold-coated flat substrate (without pattern features) to gain insight into the effects of the micropattern on the SERS enhancement. Our results show an approximate five times signal increase when R6G is adsorbed onto the gold micropatterned arrayed substrate. The effect of pattern separation distances ( $d_{\text{sep}}$ ) on the SERS signal was also investigated.



## Experimental Methods

### **Micropatterned Substrates**

Photolithography was the chosen fabrication method for preparation of the micropatterned substrates. First, glass substrates underwent an automated cleaning procedure to remove surface impurities. Patterning was carried out with the use of a bilayer resist profile comprised of a lift off resist (LOR) and a positive photoresist. Once cleaned, the substrate is spin coated with the LOR and the deposited LOR is soft baked on a hotplate. Positive photoresist is spun on top of the LOR layer and soft baked in a convection oven. The substrate is then exposed to UV light and developed via spin developing followed by a hard bake. The micropatterned glass was cut into 10 mm x 10 mm individual substrates prior to gold deposition.

### **Spherical Gold Nanoparticle Solution**

A colloidal suspension of gold nanoparticles was synthesized using a well-known citrate reduction method.<sup>5</sup> Particle size was controlled by the volume of reducing agent administered to the gold salt solution during synthesis.

### **UV-Visible Transmission**

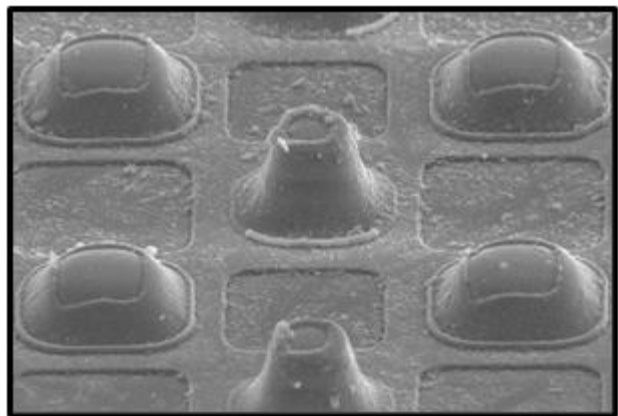
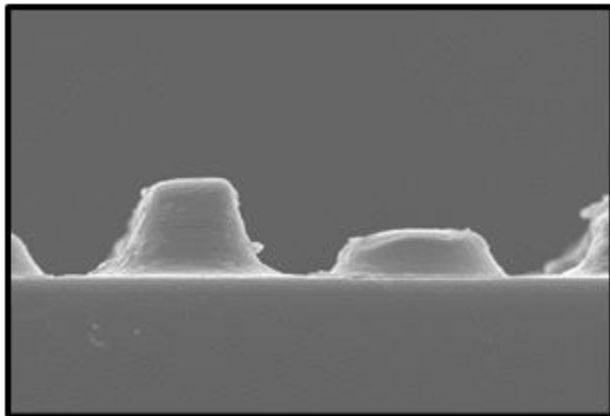
A UV-Vis light source (Ocean Insight Halogen HL-2000) and miniature spectrometer (Ocean Insight Flame UV-Vis) were used for collection of the transmission spectra. For comparison, each sample spectrum was collected under the same detection parameters

### **Spherical Gold Nanoparticle Layer**

Using a non-lithographic self-assembly technique, gold layers were developed directly on the substrates following an in-situ ligand exchange at room temperature. Coated substrates dried overnight at room temperature.

### **Surface Enhanced Raman Scattering (SERS)**

SERS measurements were carried out using an Ocean Insight 785 nm QE Pro Raman system. A 10  $\mu$ L volume of R6G sample was administered to the micropatterned substrate and allowed to dry before laser excitation. The samples were interrogated at 20 mW laser power and 3 second integration time. For comparison, each sample spectrum was collected under the same detection parameters.



**SEM images of a micropatterned surface and cross-sectional.** Self-assembled gold layers are formed within the surface volume areas of the arrayed structure and atop individual pattern features.

## Results and Discussions

### Light Deflection Properties: Transmission Spectroscopy

To gain insight into the optical effects introduced by the micropatterned structures, the transmission spectrum (Figure 1) was collected for three substrates which were fabricated with increasing feature separation distances ( $d_{sep}$ ). As expected, without the extinction properties of the gold nanoparticles, the patterned substrates transmit a large portion of the incident light (~ 90 %) in the visible wavelength range 375 nm - 700 nm. The results show that the micropatterned glass highly transmits the visible region but deflects portions of the incident UV light at ~ 400 nm and NIR light at ~ 875 nm due to the diffractive behavior of the patterned structures.<sup>6</sup> The direct light deflection is such that the photonic microstructures maintain similar spectral features while simultaneously undergoing distinct changes

in transmittance within the spectral range ~ 575 nm – 825 nm. The transmission of the substrate decreases as the spacing between adjacent pattern features increase with  $d_{8.4}$  having the highest transmission percentage and  $d_{14}$  transmitting the least. Figure 2 displays a linear correlation between the pattern structure dimensions and the transmission percentage observed at 800 nm. The NIR wavelength, 800 nm, was monitored because the scattered light at this wavelength is close to resonance with the SERS excitation source (785 nm) and the localized surface plasmon resonance (LSPR) of the coupled nanoparticles. Here, the light deflection properties of the uncoated substrates are directly related to the structure of the micropatterned surface. The photonic microstructures embedded into the glass consists of spectrally selective and highly transparent diffractive optical elements.<sup>6</sup>

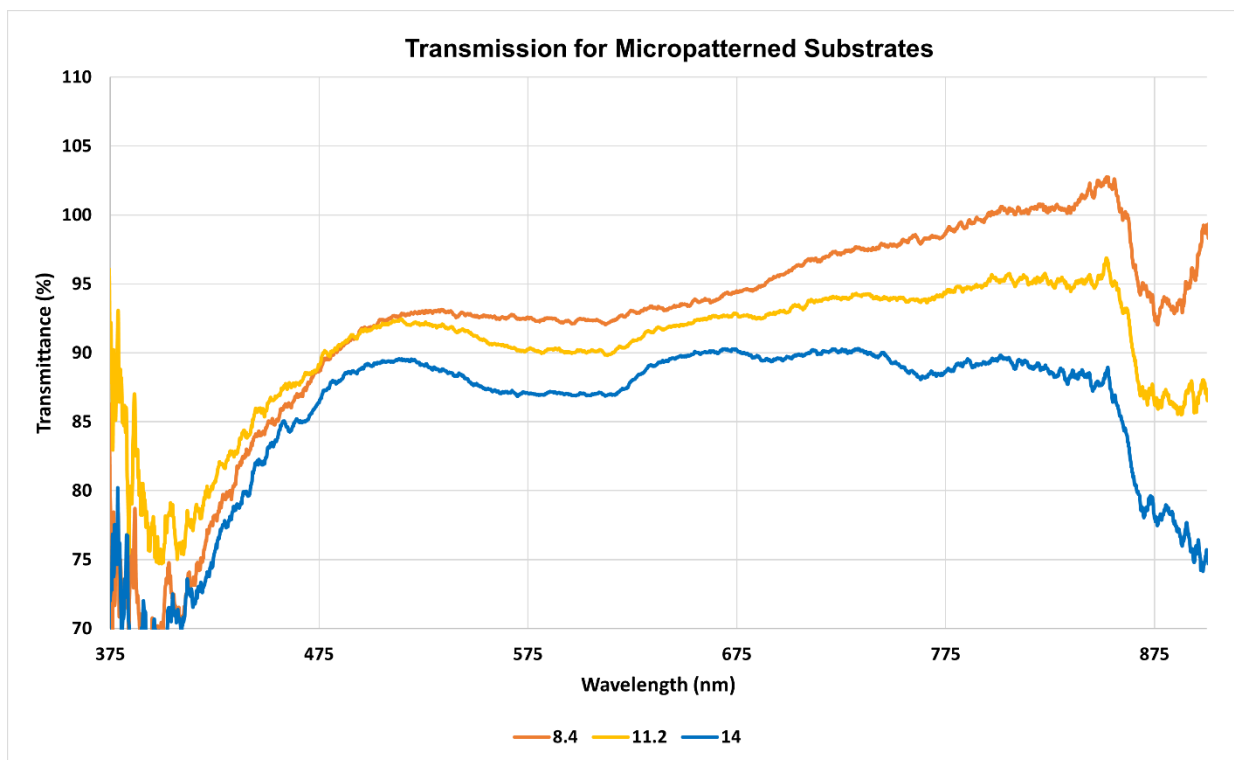


Figure 1. Transmission spectrum for three patterned substrates (left). The values 8.4, 11.2, and 14 represent an increasing distance between neighboring features.

The micropatterned substrates underwent a wet-chemical gold coating procedure where gold layers were formed directly on each substrate. This procedure was inexpensive, simple, and preserved the integrity of the gold film after drying. We propose that the self-assembled gold layers are formed within the surface volume areas of the arrayed structure and atop individual pattern features.<sup>4</sup> The transmission spectrum (Figure 3A) was collected following the gold deposition procedure to gain insight into the optical effects brought on by filling the pattern volume spaces with the metal nanoparticles. Layered gold significantly reduces the transmission for the coated micropatterns (~ 4 %). The spectrum for the gold coated structures was multiplied by eight for visual comparison to the transmission of the uncoated substrate (Figure 3A). There also appears to be broad absorption + scattering features at ~ 450 nm and ~ 800 nm. Assembly of nanoparticles into dimers, trimers and higher aggregate structures produces a coupled plasmon resonance in the NIR.<sup>7,8</sup> This is likely the case with the gold nanoparticles assembled on the micropatterned structures. The resulting surface is proposed to be a micropatterned substrate with a high density of nanoparticles producing roughened surfaces.

The transmission spectrum was collected for all three-gold coated micropatterned substrates to further examine the geometric pattern and spacing effects on a now roughened, plasmonic surface (Figure 3B). All the gold coated substrates have similar spectral features, absorption + scattering at ~ 450 nm and ~ 800 nm. The feature at ~ 800 nm suggests that the nanoparticles are forming interparticle interactions on all three patterns, resulting in a broad plasmon resonance absorption + scattering feature. This knowledge is essential to achieve successful SERS excitation by pumping this NIR LSPR. Additionally, a decrease in transmissivity with increasing pattern spatial separation is observed. This decrease in transmission is likely caused by an increase in light

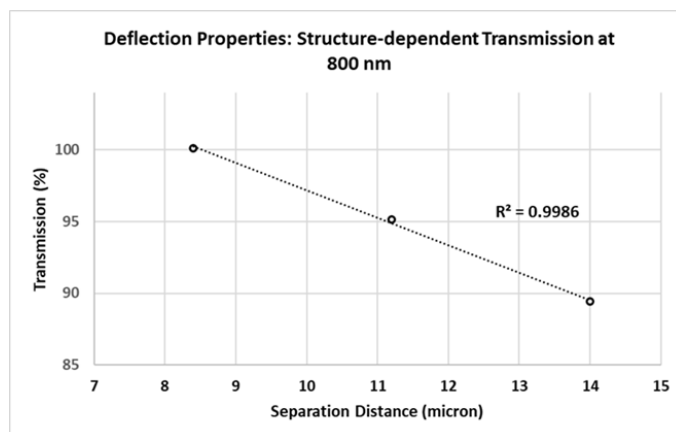


Figure 2. Transmission percentage as a function of feature separation distance. The data is best fit with a linear function resulting in a coefficient of determination,  $R^2 = 0.9986$

deflection sites provided by greater-spaced features (Figure 2). The transmission spectra provided insight into the structure-dependent deflection properties and the additional extinction properties provided by the gold nanoparticles. Importantly, this data exemplifies the ability to tune the light deflection properties of the overall substrate by altering the lateral spacing distances involved in the patterned microstructures. The tunable light deflection properties offered by the gold coated micropatterned surface is expected to function well as a SERS sensing substrate for molecular detection.

### **Chemical Sensing Performance: Surface Enhanced Raman Scattering Spectroscopy**

The SERS performance of the gold coated micropatterned substrates was investigated and compared to the signal enhancement achieved on a gold coated flat surface. The Rhodamine 6G (R6G) molecule served as the Raman probe molecule, where surface interactions occur between the positively charged moieties of the R6G molecule and the negatively charged citrate molecules at the surface of the gold nanoparticles. SERS measurements were performed utilizing

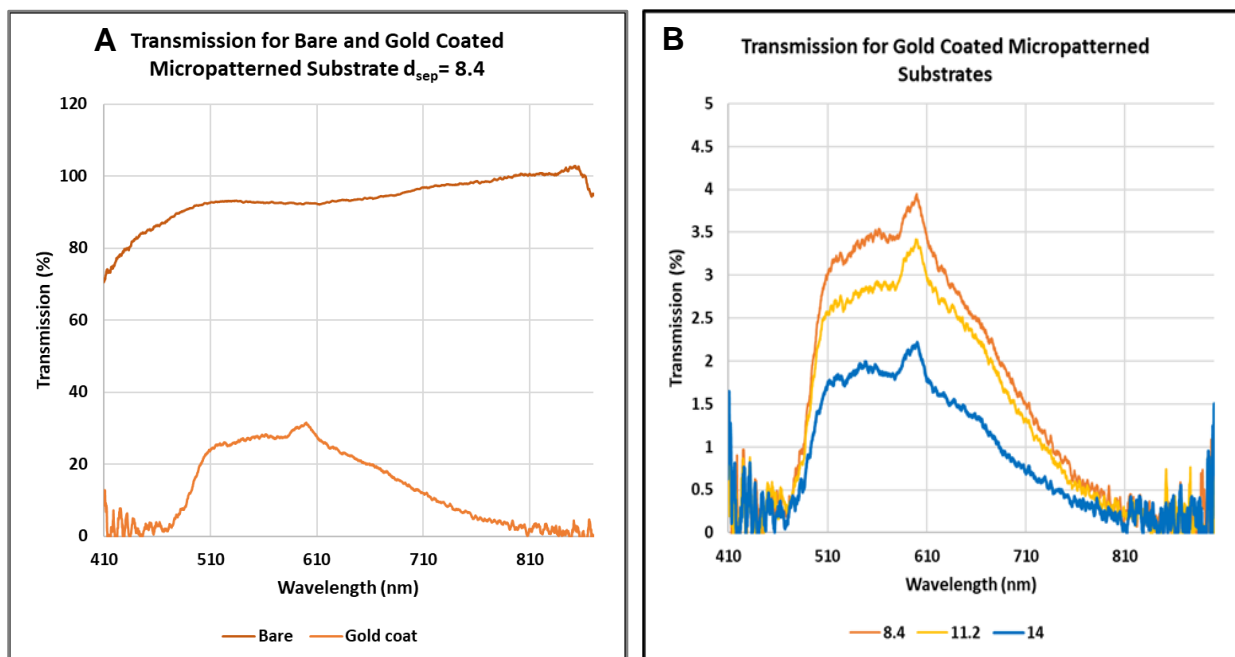


Figure 3. (A) Transmission spectra for bare micropatterned substrate and the micropatterned gold coated substrate. The transmission for the gold coated substrate has been magnified for comparison. (B) Transmission spectrum for micropatterned surfaces of varying pattern separation distances ( $d_{sep}$ ).

785 nm excitation to pump the observed LSPR for gold coated micropatterns at  $\sim 800$  nm therefore generating concentrated electromagnetic fields or “hot spots” for Raman signal enhancement. Figure 4 provides a comparative plot for R6G SERS performance on the patterned and flat surfaces. Overall, the gold coated diffractive microstructures provide an environment more conducive to Raman scattered light enhancement. In this case, the micropatterned substrate gains an enhanced signal five times greater than that of the flat surface. The following are being investigated as potential contributions to this superb micropattern-enhanced sensing:

- A) Greater surface area for molecular adsorption onto the gold nanoparticles.<sup>4</sup>
- B) Discrete structural features, such as corners and indentations, creating close-proximity nanoparticles and a higher concentration of localized “hot spots”.<sup>9</sup>
- C) Photonic microstructures selectively deflecting NIR photons creating multiple scattering events.<sup>6</sup>
- D) Preferential geometrical orientation of R6G molecules at the adsorption sites with higher localized electromagnetic fields.<sup>10</sup>



To examine the influence of micropattern dimensions on the sensing performance, the SERS spectrum was collected for R6G loaded onto each micropattern. Figure 5 displays a truncated spectrum plotted from  $1250\text{ cm}^{-1}$ – $1675\text{ cm}^{-1}$  where the general trend across the entire spectrum is that the SERS signal increases with increasing feature separation distance. The substrate with the greatest pattern separation (Figure 5, blue trace),  $d_{14}$ , provided the highest SERS enhancement for the adsorbed R6G molecules.

In Figure 5, the bands at  $1506\text{ cm}^{-1}$ ,  $1357\text{ cm}^{-1}$ , and  $1307\text{ cm}^{-1}$  represent a structure-dependent nonlinear signal intensity trend that continues at energies lower than  $1307\text{ cm}^{-1}$ . However, the band at  $1600\text{ cm}^{-1}$ , associated with vibrations occurring at the phenyl ring with  $\text{COOC}_2\text{H}_5$ ,<sup>11</sup> and the band at  $1646\text{ cm}^{-1}$ , representing a C-C stretching mode in the xanthen ring<sup>11</sup> (Figure 5, inset), appear to follow a different trend compared to the nonlinear, structure-dependent signal observed at lower energies. The correlation function describing the structure-dependent SERS signal is specific to certain vibrational modes, and therefore specific bonds. This is encouraging as it demonstrates the sensitivity of micropatterned SERS substrates to sense the unique local environment experienced by different bonds comprising the molecular structure.

The quantitative relationship between the SERS signal and the pattern ( $d_{\text{sep}}$ ), value is band specific therefore we applied a linear fit to all the structure-dependent SERS data for the vibrational modes at  $1307\text{ cm}^{-1}$ ,  $1357\text{ cm}^{-1}$ ,  $1506\text{ cm}^{-1}$ ,  $1600\text{ cm}^{-1}$ , and  $1645\text{ cm}^{-1}$  and monitored the resulting coefficient of determination values (Figure 6). The relatively poor  $R^2$  values obtained by monitoring the bands at  $1307\text{ cm}^{-1}$ ,  $1357\text{ cm}^{-1}$ , and  $1506\text{ cm}^{-1}$  points to the requirement for a nonlinear correlation function to describe the structure-dependent environmental sensing at those bonds.

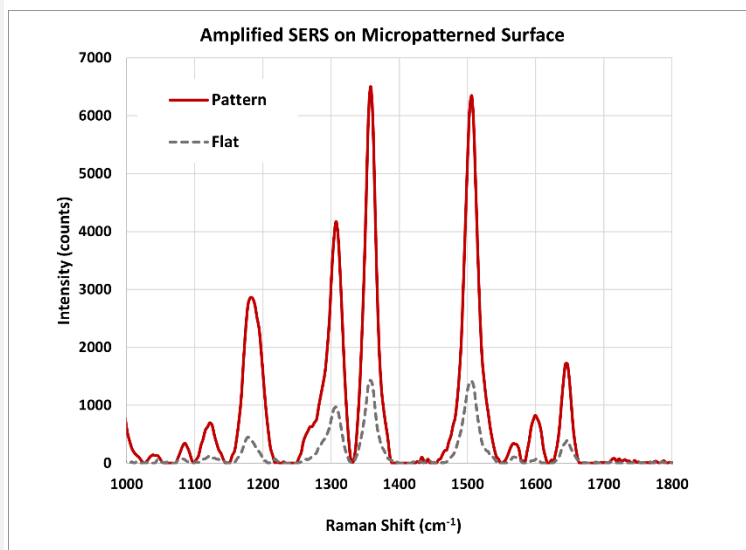


Figure 4. SERS spectra for R6G molecules adsorbed onto a gold coated flat surface (grey, dashed) and a gold coated patterned surface (red).

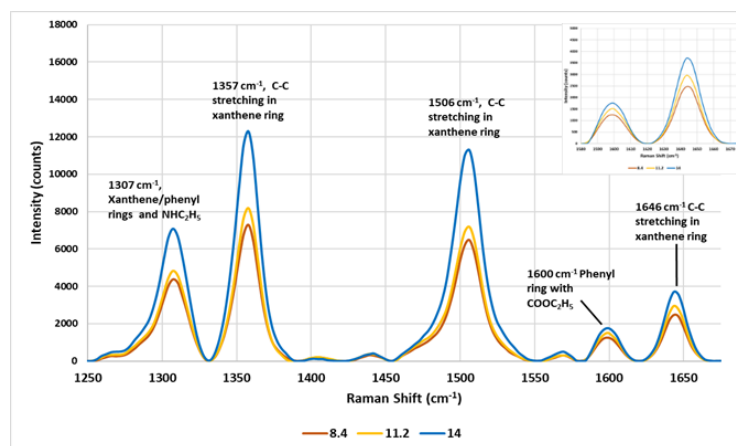


Figure 5. SERS spectra and vibrational assignments for R6G molecules adsorbed onto each micropatterned substrate. Each spectrum is the average of three experiments for each system.

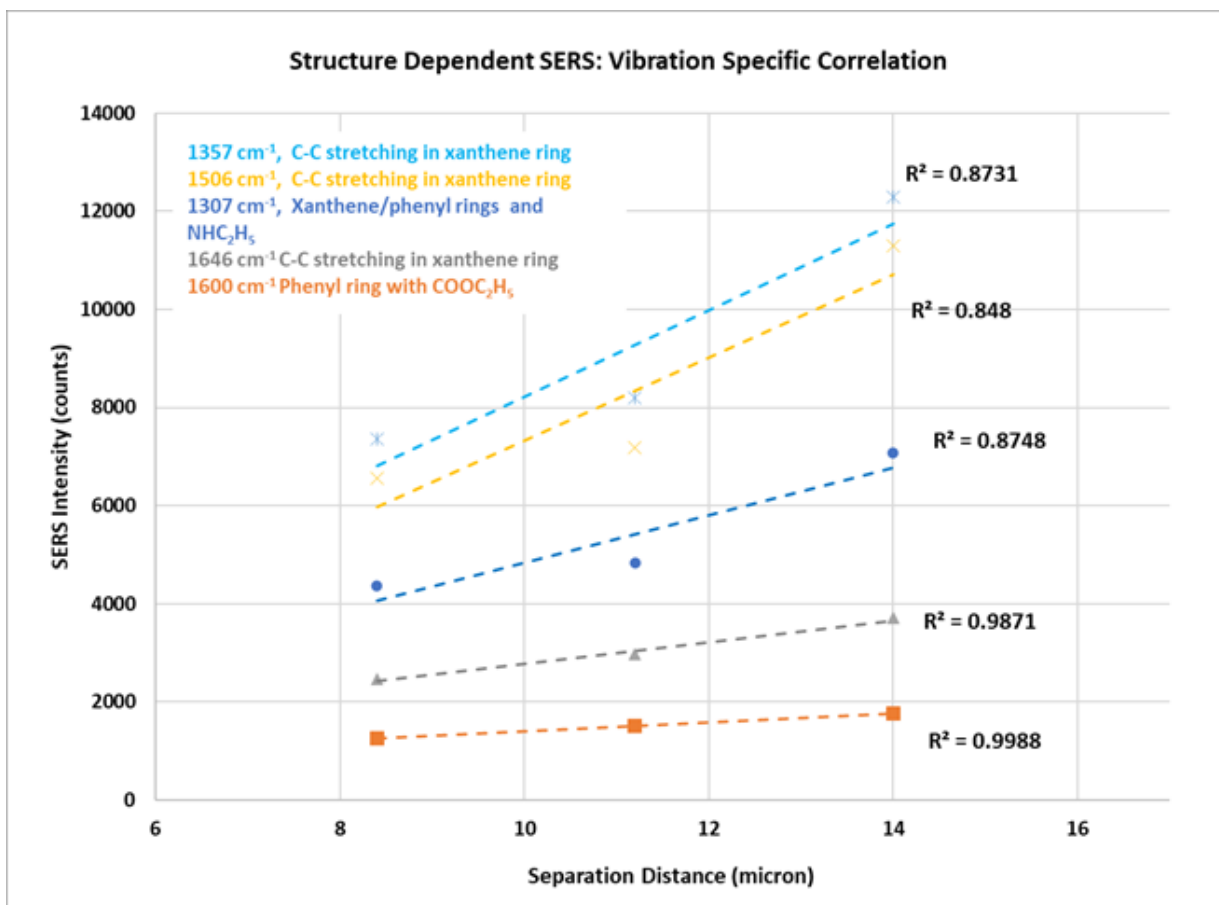


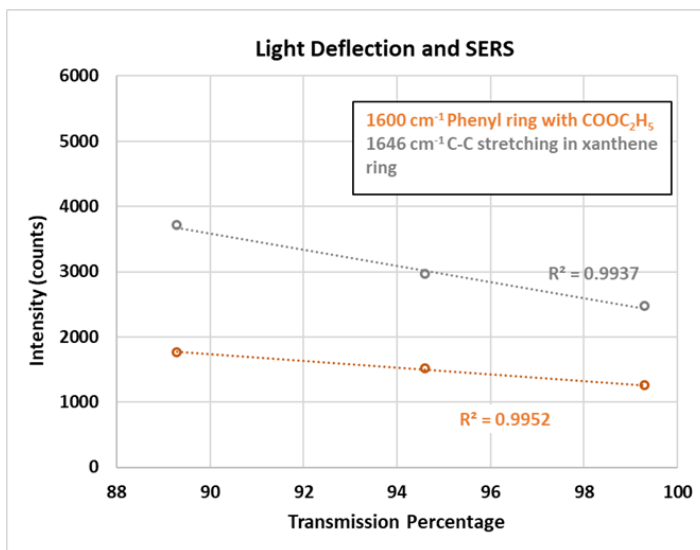
Figure 6. SERS signal intensity as a function of the micropattern feature separation distance. A linear fit was applied to all data sets and the corresponding  $R^2$  value is reported.

A structure-dependent linear correlation is best monitored using the bands at  $1600\text{ cm}^{-1}$  (orange, square) and  $1646\text{ cm}^{-1}$  (grey, triangle), representing the phenyl ring with  $\text{COOC}_2\text{H}_5$  and the stretching mode in the xanthene ring, respectively. For sensing purposes, we find that the R6G vibrational modes at  $1600\text{ cm}^{-1}$  and  $1646\text{ cm}^{-1}$  prove to be promising spectroscopic handles for microstructure-dependent environmental sensing.

Earlier we demonstrated that the structural separation distances also affected the deflection properties where greater distanced structures had a lower transmission percentage and deflected more NIR light. The linear relationship observed in Figure 2 shows a systematic trend for the structure-dependent deflection properties. A significant correlation between the deflected light of the photonic microstructures and SERS signal is interpreted in a SERS-dependent transmission percentage plot for the  $1600\text{ cm}^{-1}$  and  $1646\text{ cm}^{-1}$  bands (Figure 7). It is clear that as the greater spaced pattern substrates, like  $d_{14}$ , deflect more NIR light, the SERS signal is further increased. We propose a contributing mechanism which involves enhanced SERS scattering in the vicinity of multiple NIR light deflection events. The proposed mechanism involved in the scattering and SERS properties of the photonic microstructures is being further investigated for applicability in more complex chemical systems.

## Conclusion

In this study, we have fabricated and implemented gold coated micropatterned surfaces as SERS sensing substrates. Our results have shown that the structure-dependent SERS signal and the structure-dependent light deflection properties are bond specific. This overall sensitivity is very promising as it can be tuned by controlling the dimensions of the pattern structures and therefore tailorable for specific chemical systems.



## References

1. Kuncicky DM, Christesen SD, Velev OD. Role of the Micro- and Nanostructure in the Performance of Surface-Enhanced Raman Scattering Substrates Assembled from Gold Nanoparticles. *Applied Spectroscopy*. 2005;59(4):401-409. doi:10.1366/0003702053641559
2. Zheng H, Chen B, Yu H, et al. Microwave-assisted hydrothermal synthesis and temperature sensing application of Er<sup>3+</sup>/Yb<sup>3+</sup> doped NaY(WO<sub>4</sub>)<sub>2</sub> microstructures. *Journal of Colloid and Interface Science*. 2014;420:27-34. doi:10.1016/j.jcis.2013.12.059
3. Wycisk M, Tönnesen T, Binder J, Michaelis S, Timme H-J. Low-cost post-CMOS integration of electroplated microstructures for inertial sensing. *Sensors and Actuators A: Physical*. 2000;83(1-3):93-100. doi:10.1016/S0924-4247(00)00295-8
4. Wang Y, Wang M, Sun X, et al. Grating-like SERS substrate with tunable gaps based on nanorough Ag nanoislands/moth wing scale arrays for quantitative detection of cypermethrin. *Optics Express*. 2018;26(17):22168. doi:10.1364/oe.26.022168
5. Lee PC, Meisel D. Adsorption and surface-enhanced Raman of dyes on silver and gold sols. *The Journal of Physical Chemistry*. 1982;86(17):3391-3395. doi:10.1021/j100214a025
6. Vasiliev M, Alghamedi R, Nur-E-Alam M, Alameh K. Photonic microstructures for energy-generating clear glass and net-zero energy buildings. *Scientific Reports*. 2016;6(1). doi:10.1038/srep31831
7. Axelevitch A, Apter B, Golan G. Simulation and experimental investigation of optical transparency in gold island films. *Optics Express*. 2013;21(4):4126. doi:10.1364/oe.21.004126
8. Fediv VI. Therapeutic application of gold nanoparticles. *Clinical & experimental pathology*. 2017;16(1). doi:10.24061/1727-4338.xvi.1.59.2017.42
9. Shiohara A, Wang Y, Liz-Marzán LM. Recent approaches toward creation of hot spots for SERS detection. *Journal of Photochemistry and Photobiology C: Photochemistry Reviews*. 2014;21:2-25. doi:10.1016/j.jphotochemrev.2014.09.001
10. Williams LJ, Dowgiallo A-M, Knappenberger KL. Plasmonic nanoparticle networks formed using iron porphyrin molecular bridges. *Physical Chemistry Chemical Physics*. 2013;15(28):11840. doi:10.1039/c3cp51420j



## FAQs

### What lithography capabilities do you have?

We use lift off and etch back lithography techniques with both positive and negative resists to result in pixelated arrays, stripe filters, reticle patterns, and other customized geometries depending on the product on glass or semiconductor substrates.

### How do you make a lithography pattern?

Specifically, we use photolithography techniques with a general process outline of deposition of resist, solvent curing bake, expose, and develop, and lift off or etch back depending on the strategy and the goal.

### Can you adjust the geometries of the pattern in process?

Yes, the shape of pixels can be finely tuned by adjusting the parameters within the lithography process steps. For example, a masked square pixel could be adjusted to be more circular and smooth or more squared, which will change the surface area and topography we have created on the substrate.

